Pflügers Arch (1988) 411:137–146

Pflügers Archiv
European Journal of Physiology

Patch-clamp techniques for time-resolved capacitance measurements in single cells

Manfred Lindau [1] and Erwin Neher [2]

[1] Freie Universität Berlin, Fachbereich Physik, Abteilung Biophysik, D-1000 Berlin 33
[2] Max-Planck-Institut für biophysikalische Chemie, Postfach 2841, D-3400 Göttingen-Nikolausberg, Federal Republic of Germany

Abstract. Two methods are described for estimation of passive cell parameters such as membrane capacitance, membrane conductance and access resistance in tight-seal whole cell recording. Both methods are restricted in their application to cases where the cell under study can be approximated by a simple three-component network with linear properties over some voltage range. One method, referred to as the time domain technique, requires only standard electrophysiological equipment and a computer. Parameters are derived from an analysis of capacitive transients during square wave stimulation. It is readily adaptable to wide variations in experimental parameters. Particurlarly, it is equally applicable to the "slow whole-cell" configuration (access resistance in the range 100 MΩ to 1 GΩ) and to normal whole-cell measurements (access resistance typically 10 MΩ). The other method applies a sine wave command signal to the cell and employs a lock-in amplifier to analyse the resulting current signal. Two modes of operating the lock-in amplifier are described. One mode provides an output signal directly proportional to small changes in capacitance at maximum resolution (1–10 fF). The other mode, in conjunction with a digital computer, supplies estimates of all passive cell parameters, as does the time domain technique, but with a large amount of data reduction performed by the lock-in amplifier itself. Due to the special hardware, however, this method is not as flexible as the time domain technique.

Key words: Patch clamp – Capacitance – Mast cells

Introduction

Passive cell parameters have been estimated in the past for a variety of reasons, such as to study complex morphology (reviewed by Eisenberg and Mathias 1980), space clamp problems, and cable properties (Moore and Christensen 1985). For this reason a variety of techniques has been developed to perform impedance analysis (Clausen and Fernandez 1981; Fishman 1985). These techniques can also be used to study changes in surface area, which accompany many cellular processes such as neurite extension, membrane recycling, and exocytosis. We are interested in exocytosis, which can be measured electrically as an increase in membrane capacitance when the membrane of exocytotic vesicles is transiently incorporated into the plasma membrane (Jaffe et al. 1978; Gillespie 1979; Neher and Marty 1982; Neher 1986). For this purpose we have adapted techniques of capacitance measurement to the special condition of the tight-seal whole-cell recording configuration of the patch-clamp technique.

The methods we describe are relatively simple compared with the more elaborate techniques of impedance analysis referred to above. However, they are useful for the study of cells with simple geometry such as most small secretory cells, which can be accurately described by a three component network (Marty and Neher 1983).

Offprint requests to: E. Neher

Methods

Standard patch clamp techniques were employed as described by Hamill et al. (1981). Preparation of mast cells, solutions, and patch pipettes was as detailed by Fernandez et al. (1984) and Lindau and Fernandez (1986b). Experiments were performed at room temperature (23–25 °C). Electrical measurements were performed with an EPC-7 patch clamp amplifier (List-Electronics, Darmstadt, FRG).

Results

Time-domain technique

The measurement of displacement currents in biological membranes has been performed by a variety of techniques. The simplest is the time domain method, where the relaxation in response to an instantaneous perturbation is observed. Such a perturbation can be produced in various ways including charge movements induced by voltage steps (Armstrong and Bezanilla 1973) or light-induced charge displacement (Lindau and Rüppel 1985). The dielectric polarisation of a pure lipid membrane leads to a current transient in response to a voltage pulse. From the current signal the capacitance of the membrane can be determined.

Fast-whole-cell recording. In patch-clamp experiments, the event of patch disruption leading to the whole-cell configuration is indicated by the appearance of large capacitive current transients in response to voltage pulses (Hamill et al. 1981). The minimal equivalent circuit of this configuration is shown in Fig. 1a. C_s represents stray capacitances from the headstage of the patch-clamp amplifier and from the pipette. This capacitance is usually compensated in the cell-attached configuration before disrupting the patch using the fast transient cancellation circuit of the amplifier. The cell

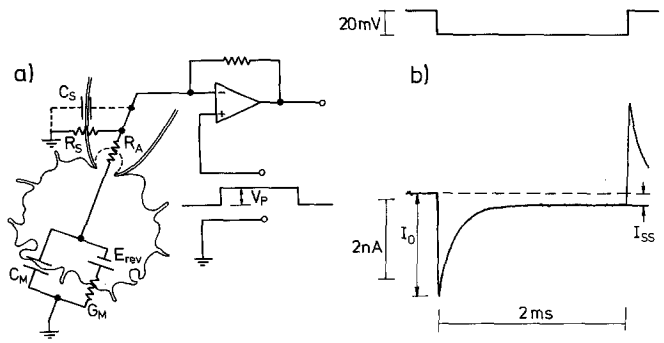

Fig. 1. a Minimal equivalent circuit of the fast-whole-cell configuration of the patch-clamp technique. The cell membrane is characterized by the parallel combination of the capacitance C_M and the conductance G_M having a reversal potential E_{rev}. R_A is the access resistance of the pipette tip. At least part of the leakage resistance (R_s) of the imperfect seal is not simply in parallel with the membrane conductance G_M. The stray capacitance C_s mainly contains contributions from the head stage of the amplifier, pipette holder and the pipette tip. This fast capacitance is compensated in the cell-attached configuration before patch disruption. **b** Current signal measured in response to a −20 mV step from a holding potential of −10 mV recorded in the fast-whole cell configuration from a rat peritoneal mast cell during degranulation. For the purpose of illustrating the steady state current an extremely leaky cell was selected. Equation (1) was fitted to the signal by a nonlinear least squares program. Equations (5–7) provided the following estimates of parameters: $C_M = 28.93$ pF, $G_M = 17.5$ nS, $R_A = 6.75$ MΩ. The signal was low-pass filtered at 29 kHz and sampled at a rate of 100 kHz. Currents I, I_o and I_{ss} were measured with respect to the baseline before the step

membrane is characterized by the membrane capacitance C_M. R_s accounts for the leakage pathway through the pipette membrane seal. The access resistance R_A ranges from 2 to 20 MΩ for typical patch pipettes (Marty and Neher 1983). The equivalent circuit of Fig. 1a, however, is valid only if the circuit parameters are independent of voltage and frequency. These conditions are not always fulfilled. Voltage dependent ion conductances are present in many cell types. In this case considerable care has to be taken that the command signals are small enough such that the nonlinearity of G_M can be neglected. In addition, the membrane capacitance may be voltage and frequency dependent due to mobile charges within the membrane (Fernandez et al. 1982). In cells with dendrites or processes parts of the membrane may be accessible only through a high series resistance and such cells must be described by more complex equivalent circuits (Moore and Christensen 1985).

In this paper we are exclusively concerned with the treatment of cells which can be described by the single time constant circuit of Fig. 1, but whose circuit parameters change slowly with time. The current in response to a voltage pulse is shown in Fig. 1 b. The capacitance of a cell is usually determined by analog compensation of the transient. This method, however, is not applicable to the measurement of a rapidly changing capacitance as in the case of granule fusion during exocytosis.

The most straightforward way to determine membrane capacitance is not to compensate the capacitive current signal and to fit an exponential to the transient according to

$$I(t) = (I_o - I_{ss}) \exp(-t/\tau) + I_{ss} \quad (1)$$

where t is the time after the voltage step. The circuit parameters are then related to the three paramenters, I_o, I_{ss} and τ through

$$R_A = \frac{V_P \cdot R_s}{I_o \cdot R_s - V_P} \quad (2)$$

$$G_M = 1 \Big/ \left(\frac{V_P \cdot R_s}{I_{ss} \cdot R_s - V_P} - R_A \right) \quad (3)$$

$$C_M = \tau \cdot \left(\frac{1}{R_A} + G_M \right). \quad (4)$$

The solutions of Eqs. (2–4) are not unique, since three measured parameters are not sufficient to calculate 4 elements of the equivalent circuit.

Therefore, certain assumptions have to be made regarding the circuit elements. If we assume the seal to be perfect. i.e. R_s to be infinitely large, Eqs. (2–4) reduce to

$$R_A^* = V_P / I_o \quad (5)$$

$$G_M^* = I_{ss} / (V_P - R_A^* \cdot I_{ss}) \quad (6)$$

$$C_M^* = \tau \cdot \left(\frac{1}{R_A^*} + G_M^* \right). \quad (7)$$

It should be noticed that Eqs. (1–7) are independent of the reversal potential of DC currents. This type of analysis can thus also be used if E_{rev} changes with time provided that such changes are slow compared to the time constant τ. Furthermore, our calculations show that the true capacitance C_M deviates from the approximate C_M^* calculated from Eqs. (5–7) by a constant scaling factor

$$C_M = C_M^* \cdot \left(1 - 2 \cdot \frac{R_A}{R_s} \right) \quad (8)$$

provided that $R_s \gg R_A$, a condition which must be fulfilled for any reasonable measurement. In the fast-whole-cell configuration the access resistance is usually in the range 2–10 MΩ. As the seal resistance R_s is normally at least 20 GΩ, the capacitance error will be less than 0.1%.

Considerable care has to be taken to exactly determine the time of the voltage step. If $t = 0$ is in error, the access resistance R_A will be in error too and this will cause errors in the determination of the other parameters [compare Eqs. (5–7)]. In particular, changes in R_A during an experiment would introduce spurious changes in the value obtained for C_M and vice versa.

We have used a PDP11/73 laboratory computer (Digital Equipment Corporation) equipped with D/A and A/D converters (Cheshire Data Interface with DT2782A, Data Translation) to generate the command pulse and to simultaneously sample the current response. The command pulse is delayed by the input filter of the patch-clamp amplifier which was switched to the 2 μs position. The built-in output filters were switched off. An 8-pole Bessel filter (902LPF2Bl, Frequency Devices, Haverhill, MA, USA) was used to filter the current before sampling at a frequency close to the Nyquist frequency. This filter introduced an additional delay of $0.506/f_c$ where f_c is the selected corner frequency. The output voltage at the D/A converter is actually changed by the computer between two sampling points. We estimated the exact time of the voltage change t_o, by systematically varying it in the analysis program. The setting at which

correlated changes in the C_M and R_A traces were minimal was subsequently used for the reconstruction. The voltage jump was thus found to occur at the pipette 4 μs after the specified number of pre-pulse sampling points. The analysis program also adds the delay introduced by the low-pass filter to obtain t_o. We have always neglected the first few data points of the current signal to avoid errors due to a slight misadjustment of the fast transient compensation. I_o is determined by extrapolating the exponential to t_o.

In the experiment of Fig. 1 b a 2 ms pulse was given and the current signal was sampled at intervals of 10 μs after low-pass filtering at 29 kHz. The time constant was about 200 μs and the time course of the capacitive transient was well resolved. The computed exponential from a nonlinear least squares fit of Eq. (1) is also drawn in this figure. It is indistinguishable from the measured signal.

If a continuous train of pulses is applied and the current signals are measured, the membrane capacitance as well as the other circuit parameters can be monitored as a function of time. The time interval between two successive pulses has to be at least 5 τ. Otherwise the current has not settled to the steady state value. In principle, the circuit parameters can be determined from the pulse-on and the pulse-off response and the inherent limit of the time resolution is thus about $5 \cdot R_A \cdot C_M$ if $R_A \ll 1/G_M$.

We have written a nonlinear least squares fitting program using the floating point buffer commands of BASIC 23. The initial guesses for the circuit parameters are computed by the program with the following expressions:

a) $G_M = 33$ pS
b) τ = pulse duration/10
c) $R_A = \tau/10$ pF .

Expression b) was used because the access resistance may vary widely between fast- and slow-whole-cell experiments (see below). It is thus assumed that an appropriate pulse duration is chosen by the experimenter. These assumptions lead to initial guesses for I_o and I_{ss} according to Eqs. (5) and (6). The program always takes the results of the last fit as the initial guess for the next signal. The average computation time per pulse (195 data points) is about 1 s. The time course of a mast cell degranulation can usually be well resolved by about 500 fits which require less than 10 min. Some signals may be distorted by artifacts. For these records the fit may be divergent or may lead to erroneous results. For this reason the program terminates the fitting if one of the following conditions occurs:

a) Convergence is not reached
b) τ becomes smaller than the sampling interval .

The fitting of the next record then starts with the initial guesses described above. Erroneous fits are usually associated with a much larger standard deviation between the theoretical curve and the data points. Therefore, the standard deviation is stored in addition to I_o, τ and I_{ss} and can subsequently be used to identify and discard bad fits.

Figure 2 gives an example of the reconstruction showing the time course of the circuit parameters in a rat peritoneal mast cell. Exocytosis was stimulated by including GTP-γ-S in the patch pipette (Fernandez et al. 1984). The patch was disrupted at $t = 0$ and -20 mV pulses (3ms) were given every 56 ms. Each signal was fitted according to Eq. (1). The reconstruction of Fig. 2 is the result of 5,539 determinations of the whole equivalent circuit. The time course of C_M, G_M and R_A is well resolved and the values obtained for the different parameters show uncorrelated changes indicating that they were well separated using this method. The noise level in the capacitance trace was ± 38 fF rms in this experiment, which is only about 0.4% of the initial total capacitance.

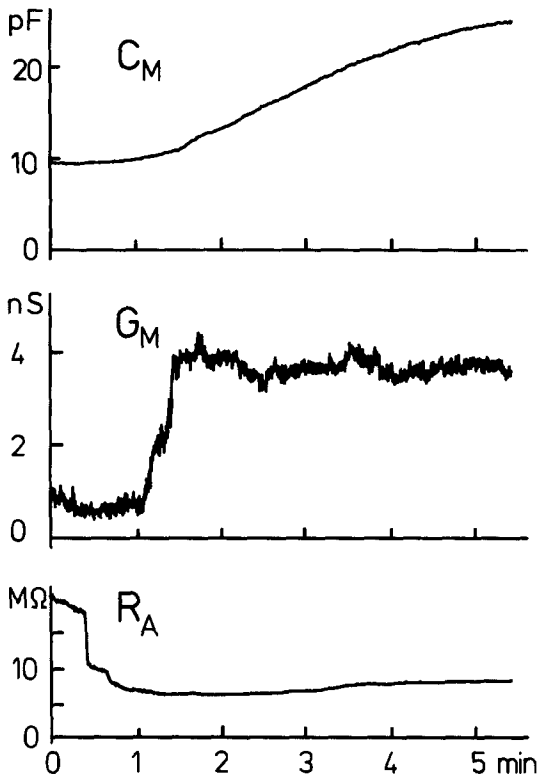

Fig. 2. Reconstruction of the cell parameters during exocytosis of a rat peritoneal mast cell. The patch was disrupted at $t = 0$. A -20 mV 3 ms pulse was given every 56 ms from a holding potential of -10 mV. 5,939 pulses were given and each response was fitted according to Eq. (1). C_M, G_M and R_A all changed considerably during the experiment. However, these changes occurred at very different times and did not induce measurable artifacts in the other traces. This experiment is not typical but has been selected to demonstrate large changes of all equivalent circuit elements. The membrane conductance normally shows only a small slow increase. Bath solution: 140 NaCl, 5 KCl, 1 $MgCl_2$, 2 $CaCl_2$, 10 HEPES/NaOH pH 7.25. Pipette solution: 150 K-glutamate, 7 $MgCl_2$, 0.5 Na_2ATP, 1.2 Tris-Cl, 0.5 BAPTA, 0.05 GTP-γ-S, 10 HEPES/NaOH pH 7.4. All concentrations in mM

The time domain analysis of the cell's equivalent circuit enables us to simultaneously track large capacitance and conductance changes at high resolution without any additional instrumentation. It is thus a convenient method to investigate the involvement of ion channels in stimulus secretion coupling. The fusion of single granules with the plasma membrane typically results in a capacitance increase of 10 – 20 fF (Neher and Marty 1982; Fernandez et al. 1984). However, to detect such small capacitance changes with this method it would be necessary to average more than 100 consecutive capacitance determinations and this would lead to a greatly reduced time resolution.

Slow-whole-cell recording. The fast-whole-cell configuration cannot be used to the study of receptor-stimulated exocytosis

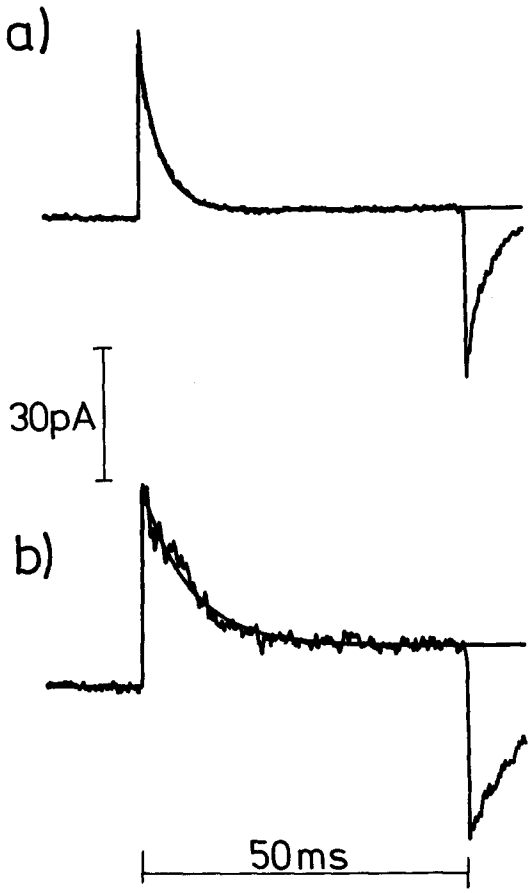

Fig. 3a, b. Time domain measurements in "slow-whole-cell" mode. **a** Current signal measured in response to a voltage pulse (20 mV) from a holding potential of −30 mV recorded in the slow-whole-cell configuration from a rat peritoneal mast cell. Equation (1) was fitted to the signal by a nonlinear least squares program (*smooth line*) giving the following cell parameters if the leakage pathway (R_S) is neglected: $C_M = 6.34$ pF, $G_M = 69$ pS, $R_A = 515$ MΩ. The signal was filtered at 4 kHz and sampled at a rate of 8 kHz. **b** Example of a distorted noisy signal recorded in the slow-whole-cell configuration. Such distortions presumably arise from the opening and closing of channels in the cell membrane or of pores within the patch during a single pulse

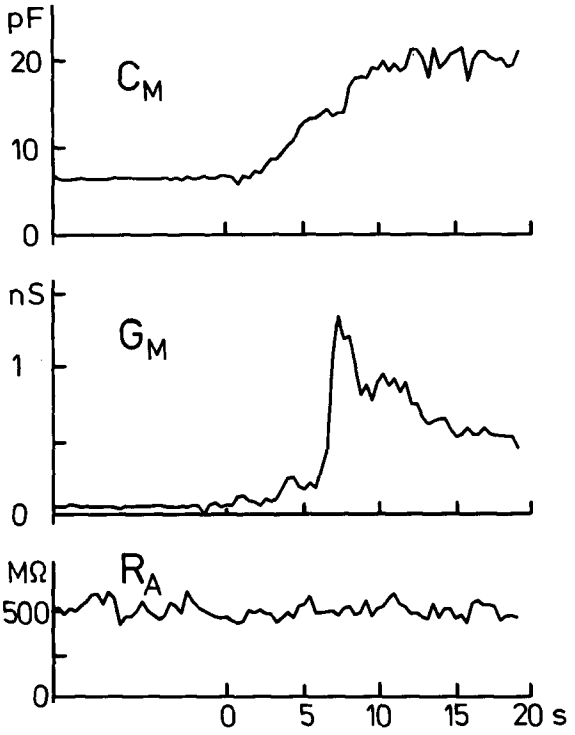

Fig. 4. Reconstruction of the cell parameters during exocytosis recorded from a rat peritoneal mast cell in the slow-whole-cell configuration. At $t = 0$ the bath solution was exchanged for a solution containing a high concentration of the secretagogue compound 48/80 (100 μg/ml). Changing the solutions took about 1 s. A 20 mV 50 ms pulse was given every 380 ms and recorded as described in the legend of Fig. 3a. The transient conductance increase occurs during the rising phase of the capacitance. The conductance changes more than tenfold without producing corresponding effects in the other traces. Bath solution (in mM): 150 NaCl, 5 KCl, 1 $MgCl_2$, 2 $CaCl_2$, 10 HEPES/NOH pH 7.23. Pipette solution: 150 K-glutamate, 20 NaCl, 1 $MgCl_2$, 0.5 Na_2ATP, 1 Tris-Cl, 10 HEPES/NaOH pH 7.2

in mast cells as the cells do not respond to this type of stimulus if dialysed with a patch pipette for some minutes (Lindau and Fernandez 1986a). This is most probably due to the wash-out of intracellular components essential for stimulus secretion coupling. The wash-out can be prevented if the patch of membrane under the pipette is only partially permeabilised instead of being disrupted by strong suction or by a voltage pulse. The patch resistance depends on the composition of the pipette filling solution (Fischmeister et al. 1986) and can be lowered by the use of pore-forming substances in the pipette (Lindau and Fernandez 1986a). This configuration has been named "slow-whole-cell" because the partial patch permeabilisation leads to a rather high series resistance and thus to a slow settling of the voltage clamp. Because of the large access resistance the capacitive transient is now much smaller and slower, but it can still be used to determine the circuit parameters (Fig. 3a), provided the pores within the patch which determine R_A are voltage independent within the range of the command signal. The duration of a pulse is now typically 50−200 ms and we have to consider the possibility that the equivalent circuit parameters may vary during a single pulse. In particular, significant changes of G_M or R_A during a pulse lead to a distorted or noisy signal as shown in Fig. 3b. Such signals are characterized by a much larger standard deviation of the fit and a reduced accuracy in the capacitance determination. This results in a much noisier capacitance trace when the time course of the cell parameters is reconstructed. On occassions we have recorded even more distorted signals which could not be fitted with a reasonable exponential and were thus discarded.

In the slow-whole-cell configuration the access resistance is usually in the range 200−1000 MΩ. The error due to the finite seal resistance R_s is now much larger. According to Eq. (8) values of $R_s = 20$ GΩ and $R_A = 1$ GΩ would lead to an error of 10% for the capacitance determination if R_s is neglected and attributed to the membrane conductance G_M. However, if the ratio R_A/R_s does not change significantly during an experiment, there will be only a constant scaling factor, and the time course as well as the relative amplitude of the capacitance change will hardly be affected. The whole-cell conductance measured in the fast-whole-cell configur-

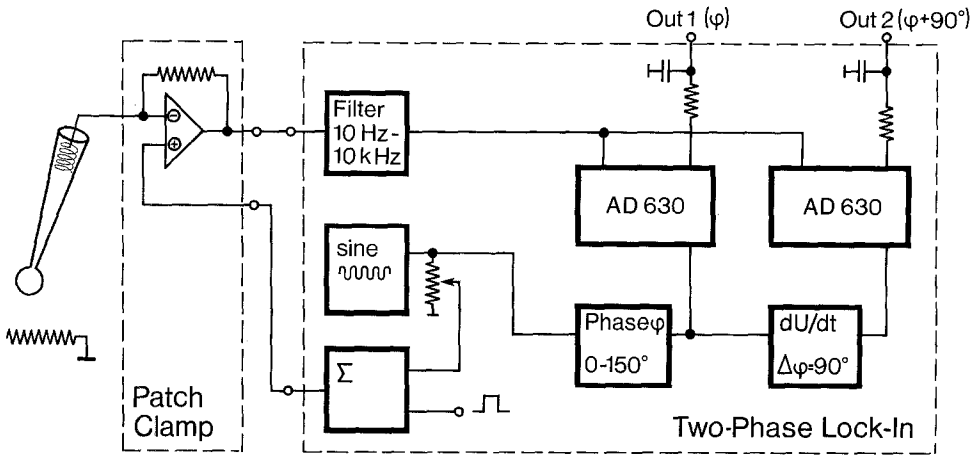

Fig. 5. Block diagram of a two phase lock-in amplifier in combination with a patch clamp apparatus. The lock-in amplifier has a built-in sine wave generator which provides a 1 V_{rms} signal, typically between 300 Hz and 1.5 kHz. A variable fraction of this signal is added to the voltage clamp command and (after 10-fold downscaling in the patch-clamp amplifier) applied to the preparation. The resulting sinusoidal current is filtered by a fixed frequency bandpass to remove spectral components outside the range of interest (DC and high-frequency noise) and then applied to two special Analog Devices circuits (AD 630) which contain most of the elements necessary for phase sensitive detection. These circuits are amplifiers with the capability of fast gain switching between +1 and −1. The gain is set by a comparator input which senses the polarity of the signal applied to it. The comparator input corresponding to "*Out 1*" is driven by the reference signal (1 V sine wave), after phase-shifting to a variable extent by a simple phase-shifter (see Horowitz and Hill 1980). The signal to the comparator input corresponding to "*Out 2*" is further phase-shifted by 90° in a differentiator circuit. The output signals of the AD 630 circuits are time averaged by an RC network (usually over 100 ms) or by a more complex low-pass filter. For a qualitative understanding consider a case where ϕ is adjusted such that the reference signal after phase-shifting is in-phase with the signal from the patch clamp. Then, the left-hand AD 630 inverts the signal exactly at the time of zero crossing such that its output is always positive and the time average is maximal. The right-hand AD 630 inverts at the time of the maximum or minimum of the input sine wave, such that the averaged output is zero. For more detail see the application manual of the AD 630 and Horowitz and Hill (1980)

ation is usually below 200 pS (Lindau and Fernandez 1986b). Similar values were observed in slow-whole-cell experiments (see legend Fig. 3a). To determine the contribution of R_s and G_M to the measured conductance the patch can be disrupted at the end of a slow-whole-cell experiment and the circuit parameters be measured in the fast-whole-cell mode. The value of R_s can then be adjusted until the same capacitance value C_M is obtained from the fast- and slow-whole-cell recording. Using this procedure we determined the seal resistance in mast cells and we frequently found that the seal was better than 65 GΩ (Lindau and Fernandez 1986a).

The time resolution of the slow-whole-cell configuration is still about 5 times the time constant of the voltage clamp, and can be approximated by $5 \cdot R_A \cdot C_M$. In a typical slow-whole-cell experiment R_A is about 500 MΩ (Lindau and Fernandez 1986a). For a 10 pF cell the lower limit would thus be 25 ms. If the capacitance increases to a value of 40 pF the time resolution is about 100 ms. The reconstruction of the equivalent circuit parameters from a degranulating mast cell recorded in the slow-whole-cell configuration is shown in Fig. 4. The cell was stimulated with compound 48/80 at $t = 0$. A 50 ms pulse was given every 380 ms and the time course of the degranulation is well resolved. The noise increase in the capacitance trace after stimulation is due to significant changes in G_M during individual pulses as demonstrated in Fig. 3b. In this case the conductance transiently increased more than tenfold due to the opening of endogenous channels to a value of about 1.5 nS, but the capacitance trace did not show any significant artifacts. This clearly shows that the conductance change indeed occurred in the cell membrane and was not due to a change of the seal resistance. Equation (8) would predict that a change of R_s would have caused a corresponding change in the capacitance trace.

Measurement of passive cell parameters with a two-phase lock-in amplifier

In the previous sections a technique of estimating passive cell parameters has been presented which uses only standard electrophysiological equipment and a digital computer. Here we describe a technique adapted from standard circuit analysis which employs a phase-sensitive detector or "lock-in amplifier" in addition. The three elements C_M^*, G_M^*, and R_A^* of the equivalent circuit (Fig. 1a, neglecting R_s) can be determined by analyzing the cell's current response when a sinusoidal command signal of fixed frequency is applied to the cell together with a constant holding potential. Two quantities (amplitude and phase or amplitudes at two mutually orthogonal phases) together with the holding current are sufficient to determine the three unknowns. The underlying assumption again is that the cells' properties are linear at least in the range of voltages covered by the sinusoidal signal. In addition, it has to be assumed that the reversal potential of DC currents is either zero (Fig. 1a) or else that it is known. A simple and very sensitive way to extract the information from the sinusoidal component uses the "lock-in" (or phase sensitive amplifier. This type of amplifier has in the past been used extensively in circuit analysis and in spectroscopy (Horowitz and Hill 1980). A simple version of such an instrument can be conveniently built from standard operational amplifiers and from a special Analog Devices circuit as detailed in Fig. 5. It provides two outputs Y_1 and Y_2 (out 1 and out 2 in Fig. 5) that are proportional to the sinusoidal components at two orthogonal phases ϕ_1 and ϕ_2 averaged

over a fixed integration time. ϕ_1 can be set to a value between 0 and 150°, while Y_2 is always 90° phase-shifted with respect to Y_1.

Use of a lock-in amplifier is the method of choice for high-resolution measurement of small changes in C_M and G_M, since it minimizes background noise. Discrete changes in capacitance related to the exocytosis of single secretory vesicles were recorded with this technique (Neher and Marty 1982; Fernandez et al. 1984). In combination with a computer this method may also be employed to monitor the time course of passive cell parameters. With appropriate selection of the lock-in frequency, degranulation of a mast cell can be monitored, although resolution of R_A and C_M is somewhat limited before and after degranulation, respectively (see below).

Computer-aided reconstruction of passive cell parameters. Considering the equivalent circuit of Fig. 1a the complex admittance Y of the cell-pipette combination at the angular frequency ω can be written as follows (we neglect R_s, use G_A instead of $1/R_A$ for convenience of notation and drop the asterisks in G_M^*, C_M^* and R_A^*).

$$Y(\omega) = G_A(G_M + i\omega C_M)/(G_M + G_A + i\omega C_M) \quad (9)$$

$$Y(\omega) = A + iB, \quad (10)$$

where

$$A = b \cdot (1 + x^2 a)/(1 + x^2 a^2) \quad (11)$$

$$B = b\,x(1 - a)/(1 + x^2 a^2) \quad (12)$$

with

$$b = 1/(1/G_A + 1/G_M); a = b/G_A; x = \omega C_M/G_M. \quad (13)$$

These expressions also neglect the pipette capacitance C_S, which, however, is compensated in the experiment.

Also

$$I_{DC} = U_{DC} G_A \cdot G_M/(G_A + G_M) = U_{DC} \cdot b \quad (14)$$

where I_{DC} is DC-current and U_{DC} is DC-voltage. Three measured quantities are available, which allow the calculation of the three unknowns G_A, G_M and C_M (Pusch and Neher 1988):

$$G_A = A + B^2/(A - b) \quad (15)$$

$$G_M = b \cdot G_A/(G_A - b) \quad (16)$$

$$C_M = 1/\omega \cdot G_A^2/(G_A - b) \cdot (A - b)/B. \quad (17)$$

In Eq. (14) it was assumed that the reversal potential E_{rev} is zero. If this is not the case U_{DC} has to be replaced by the driving force $U_{DC} - E_{rev}$.

If the phase angle of the lock-in amplifier is set to zero and capacitance of the cell is not compensated, then the output signals Y_1 and Y_2 directly provide A and B. Thus Y_1, Y_2, the DC current, and the voltage can be sampled by a computer. The quantities G_A, G_M, and C_M can then be calculated on-line and plotted as a function of time. Figure 6 shows such a recording from a mast cell, obtained with a holding potential of +25 mV superimposed upon a 16 mVrms, 810 Hz sinusoidal voltage. The DC-conductance in mast cells is quite linear with a reversal potential close to zero mV, therefore b was set equal to current divided by 0.025 V. The record shows the degranulation of a mast cell,

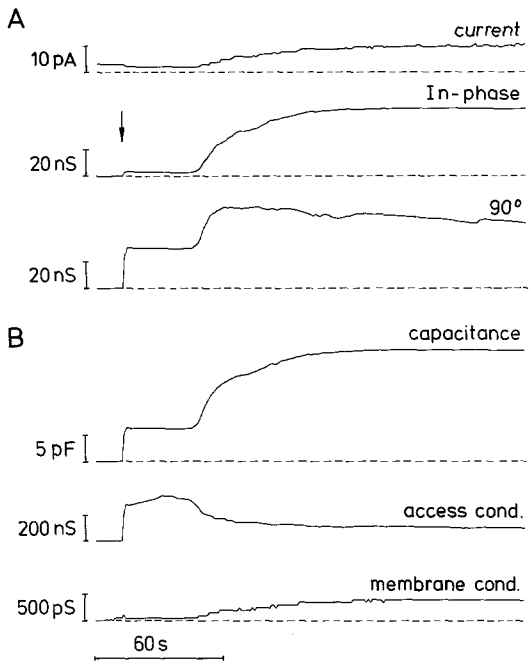

Fig. 6A, B. Computer-aided reconstruction of equivalent circuit parameters from a two phase lock-in measurement. Experimental conditions are as in Neher 1988. Lock-in parameters: 14.5 mV_{rms}, 800 Hz; 100 ms output time constant. Part **A** gives the measured quantities which are: membrane DC-current at +25 mV holding potential: in-phase signal (Y_1) and out-of phase signal (Y_2). The *arrow* marks patch rupture. Zero levels are indicated by *broken lines*. Patch rupture is marked by a pronounced increase in the out-of-phase signal. Degranulation takes place about 40 s after the start of whole-cell recording. It appears as a large increase in both lock-in signals. Part **B** gives the parameters of the equivalent circuit as calculated from the traces in **A**. For the display, sampled and calculated values were averaged over 1 s periods. Neighbouring points were connected by *straight lines*. The experiment was chosen because it illustrates that capacitance can be measured without problems in spite of large changes in G_A. It is somewhat untypical as usually changes in G_A (and correspondingly changes in the in-phase signal) are much smaller

induced by GTP-γ-S included in the pipette at 40 μM concentration.

In practice, the phase on the lock-in amplifier is actually not set to zero, but to some small value taking into account phase shifts that occur in various parts of the instrumentation, such as the built-in 10 kHz filter of the EPC-7 current monitor output or the filter of the command voltage input. It should be noted that it makes a considerable difference whether the 10 kHz or the 3 kHz output filter is selected in the patch clamp amplifier even if the lock-in frequency is in the 500 Hz to 1 kHz range. The required phase setting is most conveniently found by immersing a Sylgard-coated pipette into the bath. If C_{fast} is not grossly misadjusted the resulting signal should be purely resistive and the appropriate phase setting is that which brings the imaginary part to zero.

Finally, it should be pointed out that the measurement is only accurate if the pipette capacitance is cancelled out correctly. Very often the pipette capacitance and its associated transient is not ideally fast due to dielectric losses of the pipette and of the pipette holder. It is very important to coat pipettes with Sylgard in order to reduce these artefacts.

Contributions to the real and imaginary parts of the lock-in amplifier signal should be cancelled out in the cell-attached mode before patch rupture. For this purpose the sinusoidal signal and a DC-voltage is applied and Y_2 is zeroed by adjusting the fast capacitance compensation. Then, an offset to OUT1 (not shown in the block diagram of Fig. 5) is adjusted to zero Y_1. This procedure leaves some small errors, however. First of all, the patch capacitance (0.05–0.1 pF) is included in the compensation. It is, of course, no longer present after patch rupture. Secondly, there are three possible sources for contributions to Y_1 in the cell-attached mode. They are nonideal sealing, dielectric losses in the pipette holder and pipette, and a leaky patch. While the first two contributions should remain constant during patch rupture, this is not the case for the third one. This, however, is not readily distinguishable from the former two. Furthermore, it may happen that the seal resistance improves during the pulses which are applied for patch rupture. In any case, these errors are small for tight patches and well-coated pipettes.

In order to obtain the whole-cell configuration a pulse of suction can be applied at this point while watching the current monitor output on the oscilloscope. The sinusoidal signal increases by about an order of magnitude during patch rupture, which can be taken as an indication of having attained the whole-cell configuration.

At this time inspection of the sinusoidal current on the oscilloscope can give a rough indication whether the prerequesite of a linear current response is met. When working with electrically excitable cells, it can happen that the holding potential is not chosen low enough, such that voltage-activated channels open during the peak of the sine wave. This manifests itself as asymmetry in the current waveform. A better test – which should be routinely performed whenever changing recording conditions – is to switch off the sine wave and to apply voltage pulses, covering the voltage range of the sinusoidal command. In this test currents should be symmetrical around the holding voltage and should not show time-dependent changes, except for exponentially decaying capacitive transients. The latter transients also provide a test for the other prerequesite of the measurement, which is the validity of the three component equivalent circuit (Fig. 1a). For such a circuit the transient should be a single exponential. In order to test this, capacitance should be neutralized with the slow capacitance cancellation feature of the patch clamp amplifier. This should eliminate at least 95% of the capacitive charge. It should be noted that capacitance neutralization should be switched off again for the subsequent Lock-In measurement.

Low noise measurement. For low noise measurements the bulk of the membrane capacitance is usually neutralized, and the patch clamp amplifier is operated at high gain (typically 50 mV/pA). Compensation is needed to prevent the output signal of the patch clamp from saturating. Then, however, the simple expression for G_A, G_M and C_M given above no longer apply. Small changes in the elements of the equivalent circuit, however, can still be measured with the lock-in amplifier. The resulting changes in whole-cell current are given by:

$$\Delta I = \left(\frac{\partial Y}{\partial C_M} \Delta C_M + \frac{\partial Y}{\partial G_M} \Delta G_M + \frac{\partial Y}{\partial G_A} \Delta G_A \right) \cdot U \qquad (18)$$

where ΔI is the complex residual current after compensation, Y is the complex admittance of the equivalent circuit and U is the applied sinusoidal voltage. According to Eq. (9) the derivatives are given by (see also Neher and Marty 1982)

$$\partial Y/\partial C_M = i\omega T^2(\omega) \qquad (19)$$

$$\partial Y/\partial G_M = T^2(\omega) \qquad (20)$$

$$\partial Y/\partial G_A = (G_M + i\omega C_M)^2 T^2(\omega)/G_A^2 \qquad (21)$$

with

$$T(\omega) = G_A/(G_A + G_M + i\omega C_M) = |T| \cdot e\phi_T . \qquad (22)$$

Thus

$$\Delta I = U \cdot T^2(\omega). [i\omega \Delta C_M + \Delta G_M + \Delta G_A (G_M + i\omega C_M)^2/G_A^2] \qquad (23)$$

It is seen that apart from a phase shift of $2\phi_T$ and an attenuation factor $|T^2|$ the output signal has an imaginary part proportional to ΔC_M and a real part proportional to $\Delta G_M - \Delta G_A \omega^2 C_M^2/G_A^2$. In the latter expression it is assumed that $G_M \ll \omega C_M$. With this assumption a small contribution of the third term in Eq. (23) to the imaginary part is neglected.

If the phase angle of the lock-in amplifier is set to $2\phi_T$ its output signals Y_1 and Y_2 adopt the following values:

$$Y_1 = U|T(\omega)|^2 \cdot M[\Delta G_M - \Delta G_A \omega^2 C_M^2/G_A^2] \qquad (24)$$

$$Y_2 = U|T(\omega)|^2 \cdot M \cdot \omega \Delta C_M \qquad (25)$$

assuming that the lock-in amplifier has been internally calibrated to give 1 V maximum output for 1 V_{rms} input signal. M is the patch clamp amplifier gain in V/A. The attenuation factor $|T|$ is close to 1 if $G_A > \omega C_M$, but decreases rapidly as ω exceeds G_A/C_M. As long as $G_A > \omega C_M$ the Y_2 signal is readily interpretable as a measure of cell capacitance, whereas the Y_1 signal includes both changes in G_A and in G_M. Its interpretation requires consideration of DC conductance.

In practice both the scale factor for the capacitance signal $(U|T(\omega)^2|M\omega)$ as well as the required phase angle can be readily obtained in a given measurement by means of the calibrated capacitance neutralisation feature of the EPC-7 patch clamp amplifier. To accomplish this the capacitance of the cell is first compensated by adjusting appropriate settings of the C_{slow} and G_A potentiometers during application of square-wave pulses. Then, the sinusoidal signal is switched on and the C_{slow} setting is varied slightly about its correct value to simulate changes in membrane capacitance. At the same time the phase setting on the lock-in amplifier is slowly changed until the point is found where the Y_2 value changes maximally with changes in the C-setting, while the Y_1-value is stationary. Once this phase setting is found, the C-setting is finally changed by a fixed amount (say 0.1 pF), and the corresponding displacement of Y_2 is taken as a calibration mark for capacitance. It should be pointed out that these calibrations are valid only for small changes around the initial value after a capacitance compensation has been performed. Thus, the procedure including capacitance compensation has to be repeated whenever large changes in Y_1 and Y_2 occur.

A very serious problem often arises, when pipettes tend to seal off after formation of the whole-cell recording mode (see Fig. 6B). Changes in R_A then becomes so large that the calibration procedure has to be repeated. It may be necessary to apply another pulse of suction in order to improve the access resistance. Sometimes R_A does remain stable after

repeated attempts of this kind. Likewise, during degranulation in mast cells (Almers and Neher 1987) and high-$[Ca]_i$ stimulation in chromaffin cells (Penner et al. 1986) the compensation has to be repeatedly adjusted due to the considerable changes that occur in C_M. Examples of recordings from mast cells both with and without series resistance problems are shown in Fig. 7.

Criteria for selection of the lock-in frequency. Three important aspects of the measurement are influenced by the selection of the lock-in frequency:

(i) The signal-to-noise-ratio changes with frequency since signal and noise are both frequency dependent. Estimation of relative amplitudes suggests that the frequency should be selected in the range 500 Hz to 1.5 kHz (see below).

(ii) The required phase angle depends on frequency. However, if $\omega < G_A/C_M$ then the phase angle is small, $|T(\omega)|$ is close to unity, and the exact setting of ϕ is not critical. Therefore, the selected frequency should be as low as possible.

(iii) If ϕ is not set correctly, changes in G_M and G_A will cross over and contribute to the Y_2-singal. For an experiment where large changes in G_M or large leakage conductances are expected, a high frequency should be chosen because contributions of ΔG_M are frequency independent whereas Y_2 increases linearly with ω. If, however, changes in G_A are expected, a low frequency should be chosen because the contribution from ΔG_A increases with ω^2.

These three considerations provide conflicting recommendations for frequency selection. However, ΔG_M contributions should in practice be small, unless there is excessive leak. Thus, a compromise has to be found between the requirements of the signal/noise ratio and the effects of G_A-changes.

The noise of the lock-in measurement is given by the product of the recording bandwidth (given by the averaging time constant at the lock-in output) and the noise spectral density of the input signal at the lock-in frequency. In a whole-cell recording the dominant noise source above 200–500 Hz is that of G_A and C_M in series (Marty and Neher 1983). The spectral density in the noise power of such a combination increases with ω^2 up to the characteristic frequency $\omega_c = G_A/C_M$.

The power of the lock-in output signal also increases with ω^2 up to ω_c, at which point it starts to decrease with $1/\omega^2$ due to the influence of $|T(\omega)|^2$ in Eq. (23). Thus, the signal-to-noise ratio is constant up to approximately ω_c and falls thereafter. For example, for a cell with 10 pF capacitance and 0.1 μS (10 MΩ) series conductance, the characteristic frequency is 10^4 radians/sec or 1.6 kHz. The lock-in frequency should thus be selected between about 500 Hz and 1.5 kHz. At lower frequencies other noise sources become dominant (Marty and Neher 1983). In this range the relative resolution $\Delta C_M/C_M$ is given by:

$$\Delta C_M/C_M = \sqrt{4kTR_A\Delta f}/U \qquad (26)$$

where R_A is the access resistance, Δf is the equivalent noise bandwith set by the output filter of the lock-in amplifier, and U is the rms-value of the applied sinusoidal voltage. The right side of Eq. (26) is the ratio between the Johnson noise of the access resistance and the applied voltage. Using a model circuit, Neher and Marty (1982) measured 0.15 fF rms-noise with $C_M = 4.7$ pF; $R_A = 2$ MΩ; $\Delta f = 5$ Hz and

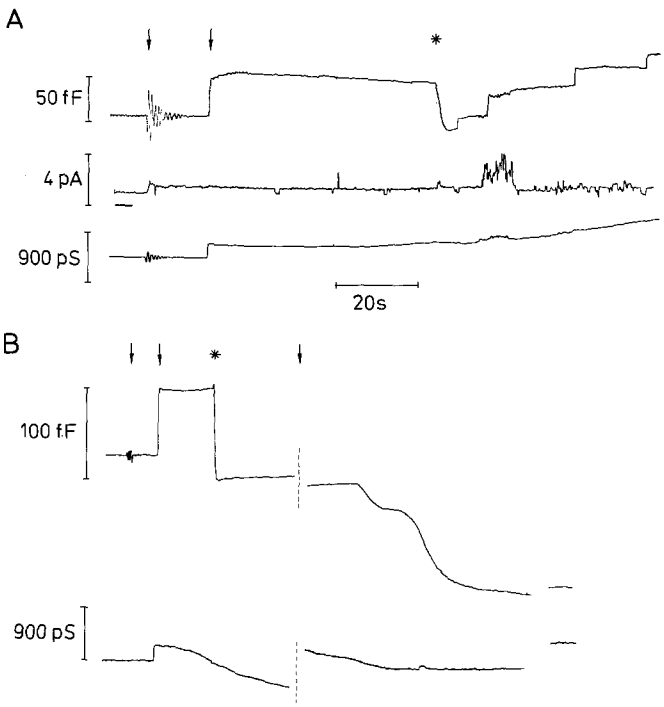

Fig. 7 A, B. High-resolution lock-in recordings on mast cells. Experimental conditions were similar to those given by Almers and Neher (1987) except that a smaller sinusoidal signal (11 mV_{rms}) was applied here. Part **A** shows the lock-in output at ϕ +90° (Y_2, uppermost trace), DC-current (*center trace*) and the lock-in signal at ϕ (Y_1, *lowermost trace*). The *first arrow* marks rupturing of the patch. Some ringing, during the first 15 seconds results from test pulses which were applied in order to compensate the bulk of the cell capacitance (6.9 pF, $G_A = 420$ nS). The *horizontal bar* below the current trace marks the zero-current level. At the time of the second arrow the sinusoidal signal was switched on to start the capacitance measurement. The break in the record at this point reflects approximately 50 fF of uncompensated capacitance. Approximately 1 min later (*) an episode of gradual capacitance decline occured (as described by Almers and Neher 1987). This was followed by stepwise increases in capacitance, resulting from fusion of individual mast cell granules with the plasma membrane. Membrane current (center trace; holding potential −30 mV; inward displayed upwards!) shows some fluctuations, partly due to channel openings, partly due to erratic leaks. Only the largest of these affect the measurement of capacitance. Access conductance (*lowermost trace*) is constant for the first 60 s and then slowly decreases (upward drift!). Membrane conductance contributes only little to this signal. This can be seen towards the end of the record, where a burst of leakage current produces only a marginal upward deflection. Part **B** shows a similar recording with some series resistance problems. Membrane current is not displayed here, because it was very small throughout. Compensated membrane capacitance in the beginning was 5.4 pF at 220 nS access conductance. At the time marked by the *asterisk* the capacitance compensation was reduced to 5.3 pF. The corresponding step in the capacitance trace can be taken as a calibration mark for 100 fF. It is seen, that the other signal is totally unaffected by the change. This proves that the phase had been set correctly. The conductance signal changed markedly during the first 60 s of the recording. At the time of the third *arrow* the G_A-setting of the patch-clamp was changed in order to restore the conductance trace to the original level. It now read 300 nS. This change also resulted in a small offset in the capacitance trace. Subsequently the cell displayed two episodes of gradual capacitance decline as described by Almers and Neher (1987). Towards the end of the record (during the break) the G_A-setting of capacitance compensation was readjusted, giving a final G_A of 380 nS. The *calibration bar* for the conductance trace refers to changes in G_M

$U = 18$ mV. This compares favourably with the prediction of Eq. (26), which is 0.11 fF. In real cells, however, the background noise is larger by about one to two orders of magnitude, as shown by Neher and Marty (1982). This is due to the fact that most cells contain ionic channels which add to the background noise, through their opening- and closing statistics, and due to quite a variety of small surface area changes in living cells which cannot be readily controlled.

Comparison between the two modes of lock-in amplifier measurement

The measurement employing cell capacitance neutralization described above has the advantage of providing a highly resolved signal for smal capacitance changes with minimal equipment needs. Plotting of Y_1 and Y_2 together with the DC-current on a chart recorder is usually adequate. It is difficult, however, to sort out combined changes in C_M, G_M and G_A. The other mode of operation, employing a computer is convenient in that it directly provides the quantities of interest. It is somewhat restricted in two respects: First, limitations in dynamic range constrain the resolution. For instance with a 12 bit AD-converter the maximum relative resolution is approximately 1 part in 10^3. Thus, for a 10 pF cell the optimum resolution is 10 fF. Secondly it may not always be possible to select an appropriate lock-in frequency when the cell parameters change over a wide range.

It is, of course, possible to combine the two modes of operation by using capacitance neutralization and calculating on-line the true cell parameters. For this, the computer program would have to know the initial as well as updated settings of the C-neutralization during the course of the measurement.

Discussion

We have described two methods for the time-resolved measurement of cell membrane capacitance and conductance. These parameters can be determined from the current relaxation in response to a voltage step or by the response to steady state sine wave stimulation. The current relaxation method for time-resolved measurements of capacitance and conductance during exocytosis is a convenient technique which can be applied in the fast- and slow-whole-cell configuration of the patch-clamp. Large changes of the access resistance are tolerated by this method and no assumptions about the value and stability of the cell's reversal potential are necessary. All experimental operations including stimulation and data aquisition are under control of the computer, which provides flexibility in adjusting experimental parameters to the specific needs of a given preparation. In the fast-whole-cell mode the capacitance resolution is better than $\pm$ 35 fF at a time resolution of milliseconds. The resolution is comparable to that obtained by transfer function measurements using a pseudo random binary sequence generator (Fernandez et al. 1984). To resolve discrete fusion events associated with a capacitance increase of 10–20 fF, it would be necessary to average about 100 capacitance values. This could be done by continuous sampling of the current in response to a 250 Hz square wave command input which would imply the storage of 10^5 data points per second over a period of minutes. The time required for analysis would be many hours.

For high-resolution studies, such as the fusion of single granules the method employing a lock-in amplifier is thus more appropriate. The lock-in amplifier in its most straightforward use provides readily interpretable signals at a resolution in the range 1 fF which can be traced out directly on a chart recorder. Alternatively it can be used to achieve a significant amount of data reduction when used in a mode similar to that of the time-domain technique. For each estimation of the circuit parameters, which typically is made every 100 ms to 1 s, the computer, in combination with the lock-in amplifier, has to sample only four values, performing the algebraic operations of Eqs. (14–17) in order to obtain estimates of the cell parameters. For the same task, using time domain techniques, the computer must supply a stimulus via the D/A and it has to sample and store on disk typically 200 data points. Subsequently, in off-line analysis, it performs an iterative least squares fit on 200 values, evaluating the fitted parameters according to Eqs. (5–7). The choice between the methods described should therefore mainly be influenced by equipment availability and by requirements of resolution and flexibility.

Acknowledgements. We would like to thank our colleagues Susan DeRiemer, Meyer Jackson, Martin Holz and Peter Tatham for numerous helpful comments on the manuscript. This work was partially supported by the Deutsche Forschungsgemeinschaft (SFB 312, Gerichtete Membranprozesse).

References

Almers W, Neher E (1987) Gradual and stepwise changes in the membrane capacitance of rat peritoneal mast cells. J Physiol 386:205–217

Armstrong CM, Bezanilla F (1973) Currents related to movement of the gating particles of the sodium channels. Nature 242:459–461

Clausen C, Fernandez JM (1981) A low-cost method for rapid transfer function measurements with direct application to biological impedance analysis. Pflügers Arch 390:290–295

Eisenberg RS, Mathias RT (1980) Structural analysis of electrical properties of cells and tissues. CRC Crit Rev Bioeng 4:203–232

Fernandez JM, Bezanilla F, Taylor RE (1982) Distribution and kinetics of membrane dielectric polarization. II. Frequency domain studies of gating currents. J Gen Physiol 79:41–67

Fernandez JM, Neher E, Gomperts BD (1984) Capacitance measurements reveal stepwise fusion events in degranulating mast cells. Nature 312:453–455

Fishman HM (1985) Relaxations, fluctuations and ion transfer across membranes. Prog Biophys Mol Biol 46:127–162

Fischmeister R, Ayer Jr RK, De Haan RL (1986) Some limitations of the cell-attached patch clamp technique: a two electrode analysis. Pflügers Arch 406:73–82

Gillespie JT (1979) The effect of repetitive stimulation on the passive electrical properties of the presynaptic terminal of the squid giant synapse. Proc Roy Soc Lond B 206:293–306

Hamill OP, Marty A, Neher E, Sakmann B, Sigworth FJ (1981) Improved patch-clamp technique for high-resolution current recording from cells and cell-free membrane patches. Pflügers Arch 391:85–100

Horowitz P, Hill W (1980) The art of electronics. Cambridge University Press, Cambridge

Jaffe LA, Hagiwara S, Kado RT (1978) The time course of cortical vesicle fusion in sea urchin eggs observed as membrane capacitance changes. Dev Biol 67:243–248

Lindau M, Fernandez JM (1986a) IgE-mediated degranulation of mast cells does not require opening of ion channels. Nature 319:150–153

Lindau M, Fernandez JM (1986b) A patch-clamp study of histamine-secreting cells. J Gen Physiol 88:349–368

Lindau M, Rüppel H (1985) On the nature of the fast light-induced charge displacement in vertebrate photoreceptors. Photobiochem Photobiophys 9:43–56

Marty A, Neher E (1983) Tight-seal whole-cell recording, In: Sakmann B, Neher E (eds) Single-channel recording. Plenum Press, New York pp 107–121

Moore LE, Christensen BN (1985). White noise analysis of cable properties of neuroblastoma cells and lamprey central neurons. J Neurophys 53:636–651

Neher E (1986) Patch clamp studies on the role of calcium in secretion. Fortschr Zool 33:275–285

Neher E (1988) The influence of intracellular calcium concentration on degranulation in dialysed mast cells from rat peritoneum. J Physiol 395 (in press)

Neher E, Marty A (1982) Discrete changes of cell membrane capacitance observed under conditions of enhanced secretion in bovine adrenal chromaffin cells. Proc Natl Acad Sci USA 79:6712–6716

Penner R, Neher E, Dreyer F (1986) Intracellularly injected tetanus toxin inhibits exocytosis in bovine adrenal chromaffin cells. Nature 324:76–78

Pusch M, Neher E (1988) Rates of diffusional exchange between small cells and a measuring patch pipette. Pflügers Arch 411:204–211

Received May 29/Received after revision September 22/
Accepted October 6, 1987

Note added in proof

The problem of washout addressed in the section on slow-whole-cell can partially be overcome by inclusion of GTP in the recording pipette (Penner R, Pusch M, Neher E (1987) Washout phenomena in dialyzed mast cells allow discrimination of different steps in stimulus-secretion coupling. Biosci Rep 7:313–321).